Bioorganic & Medicinal Chemistry Letters 20 (2010) 7250–7254

Contents lists available at ScienceDirect

Bioorganic & Medicinal Chemistry Letters

journal homepage: www.elsevier.com/locate/bmcl

Synthesis, crystal structure, DNA-binding and cytotoxicity in vitro of novel *cis*-Pt(II) and *trans*-Pd(II) pyridine carboxamide complexes

Chun-Yue Shi [a,b], En-Jun Gao [b], Shuang Ma [b], Mei-Lin Wang [b], Qi-Tao Liu [a,c,*]

[a] Faculty of Chemistry, Northeast Normal University, Changchun 130024, PR China
[b] Applied Chemistry Department, Shenyang University of Chemical Technology, Shenyang 110142, PR China
[c] College of Chemistry, Liaoning University, Shenyang 110036, PR China

ARTICLE INFO

Article history:
Received 6 June 2010
Revised 29 September 2010
Accepted 20 October 2010
Available online 26 October 2010

Keywords:
Pyridinecarboxamide
DNA-binding
Pt(II) and Pd(II) complexes
Cytotoxic activity

ABSTRACT

In an attempt to establish fundamental structure–activity relationships (SAR) of Pt/Pd-based anti-tumour compounds, we have recently designed monodentate pyridyl amide ligand containing central amide units which possess external metal co-ordinating pyridyl group and internal amide functionality. It was prepared in one step from commercially available compounds in moderate to good yield. Surprisingly, treatment of $K_2[MCl_4]$ [M = Pt(II), Pd(II)] with ligand *N*-(4-chlorophenyl)-3-pyridinecarboxamide (L) in the same reaction condition affords two different hydrogen-bonded polymers: *cis*-$[PtL_2Cl_2]\cdot CH_3OH\cdot DMF$ (**1**) and *trans*-$[PdL_2Cl_2]\cdot 2DMF$ (**2**). Fluorescence analysis indicates that the two complexes can bind to fish sperm DNA (FS-DNA) and gel electrophoresis assay demonstrates the ability of the complexes to cleave the pBR322 plasmid DNA. The two complexes exhibit cytotoxic specificity and significant cancer cell inhibitory rate. Furthermore, cytotoxicity values are higher in the case of *cis*-Pt(II) complex than *trans*-Pd(II) complex in four different cancer cell lines.

The carboxamide linkage, [–C(O)NH–], is an essential building unit in the primary structure of proteins, which has attracted much attention because it can provide models from the standpoint of bioinorganic chemistry.[1–3] Consequently, the behaviour of pyridinecarboxamide, containing this linkage, towards biologically relevant metals has been widely investigated.[4–11] This is because pyridine carboxamide ligand contains lipophilic group of aromatic ring and hydrophilic group of carboxamide. The lipophilic group can make drugs more capable of penetrating through cell membrane to bind to the target DNA, and the hydrophilic group can reduce toxicity from the drugs. Especially, the search for platinum(II) complexes with anti-tumour properties has been going on through the efforts of chemists from the medicinal chemistry field since the discovery of the anti-proliferation activity of cisplatin in the 1960s.[12] To an attempt to reduce toxicity and improve the original bioactivity of cisplatin, thousands of cisplatin analogues have been prepared and tested by varying the nature of the labile ligands (also called the leaving groups) and non-labile ligands (also called the carrier ligands). Meanwhile, for decades it is believed that *trans* platinum compounds are non-active as anti-tumour agents because transplatinum is biologically inactive although it binds to DNA. However, since the 1990s many *trans* platinum complexes have been discovered with significant anti-tumour activity against different tumour cells including these resistant to cisplatin.[13–16] Owing to the similar co-ordination modes of the cation Pd(II) and Pt(II) (d^8-electron configuration) there has also been renewed interest in attempts to obtain activity for *cis* and *trans* palladium(II) complexes.[17–21]

The aim of the studies was to broaden our knowledge on the antiproliferative activity of Pt(II)/Pd(II) complexes and understand the structure–activity relationships (SARs) of these new chemical compounds. Recently, we obtained two novel *cis*-dichloroplatinum(II) and *trans*-dichloropalladium(II) complexes containing non-chelation-controlled 3-pyridinecarboxamide derivatives as carrier groups (Scheme 1). A specific attention has been focused on the effect induced by solvent molecule on the nature of the resulting self-assembly under identical conditions. In the present Letter we describe the synthesis and characterisation of the self-assembled products, *cis*-$[PtL_2Cl_2]\cdot CH_3OH\cdot DMF$ (**1**) and *trans*-$[PdL_2Cl_2]\cdot 2DMF$ (**2**), (L = *N*-(4-chlorophenyl)-3-pyridinecarboxamide), as well as the DNA-binding abilities of them with FS-DNA via fluorescence spectroscopy. Their cleavage behaviour toward pBR322 DNA and the in vitro cytotoxicity against the human cervix epitheloid carcinoma (Hela), human hepatocellular carcinoma (Hep-G2), human oral epithelial carcinoma (KB) and human lung carcinoma (AGZY-83a) are also investigated.

According to our previous work,[22] the ligand was prepared by the reaction of nicotinoyl chloride hydrochloride with 4-chloroaniline in dry THF in presence of triethylamine under N_2 8 h (Scheme 1). The solid-state complex was obtained by mixing 2:1 molar ratio of the appropriate ligand and K_2PtCl_4 (or K_2PdCl_4) in

* Corresponding author. Tel.: +86 024 62202018; fax: +86 024 86852421.
E-mail address: qtliu@yahoo.com.cn (Q.-T. Liu).

0960-894X/$ - see front matter © 2010 Elsevier Ltd. All rights reserved.
doi:10.1016/j.bmcl.2010.10.097

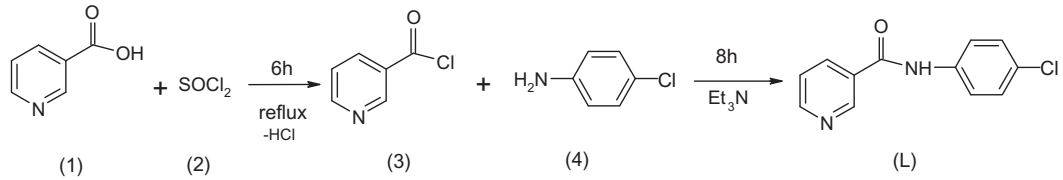

Scheme 1. The formation of *N*-(4-chlorophenyl)-3-pyridinecarboxamide (L).

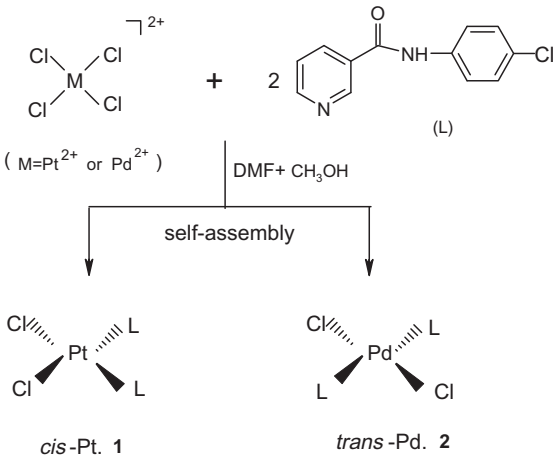

Scheme 2. The synthetic route of **1** and **2**.

methanol–water solution. The precipitate was recrystallised from the mixed solvents DMF and methanol, and orange crystals of X-ray quality were obtained and identified as complex **1** and yellow crystals as complex **2** (Scheme 2). Crystal data and structure refinement details of complexes **1** and **2** are summarised in Table S1. Selected bond lengths and angles are listed in Table S2.

The starting hypothesis for this work is that complexes with pyridine carboxamide ligands should have hydrogen bonds between the ligand NH group (as H-bond donor) and Cl atom (as H-bond acceptor) and *cis* or *trans* configuration of the complex might also arise from the influence of solvent molecule taking part in hydrogen bonding interactions. In that case, they could be used as supramolecular synthons for designing complexes with extended arrays whose shapes and bonding structures are controlled by the geometrical configuration of the synthons and direction and number of hydrogen bonds. Figure 1 shows the different intermolecular hydrogen bonding patterns of complexes **1** and **2**, respectively.

In the structure of complex **1**, each platinum atom has *cis*-$PtCl_2N_2$ co-ordination. The atoms involved in square co-ordination of Pt(II) deviate 0.037 Å from the average mean plane $PtCl_2N_2$ [Pt(1), Cl(1), Cl(2), N(1), N(3)]. Average value for Pt–Cl distances is 2.3009(17) Å while the average Pt–N distance [2.028(5) Å] is in the expected region.[8] The dihedral angle between the two phenyl rings is 65.75° and the angle between the two pyridine rings is 69.87°. Both of the molecules form hydrogen-bonded dimers with Pt...Pt distance of 4.000 Å (Fig. 1). The arrangement is supported by intermolecular H-bond between NH centre of one pyridinecarboxamide ligand and Cl atom of the neighbouring molecules (distance N(2)–H...Cl(2) is 2.620 Å) and also between NH centre of the other pyridinecarboxamide ligand and O atom of the solvent DMF (distance N(4)–H...O(3) is 2.141 Å). It is notable that these dimeric entities are interlinked to form a 2D framework via intricate hydrogen bonds with solvent DMF and methanol molecules as well as weak π–π interactions (the shortest interplanar atom–atom separation of ca. 3.906 Å) (Fig. 2a). The sheets are further connected by very weak C(1)–H...Cl(2) (2.938 Å) and C(2)–H...O(1) (2.574 Å) hydrogen bonds extending along the *a*-axis to form a 3D network.

As can be seen from Figure 1, each palladium atom also adopted square-planar geometry co-ordinated by 2 equiv pyridine nitrogen atoms [N(1) and N(1A)] from two ligands and two chloride anion [Cl(1) and Cl(1A)]. However, there are the difference in the conformation of the ligand in the palladium complex relative to the platinum complex. The two ligands are *trans* to each other (i.e., N1 is *trans* to N(1A)). The Pd–Cl bond length is 2.2995(6) Å and the Pd–N bond length (2.0129(17) Å) is that expected for normal Pd–N single-bond distance.[18] The two pyridine rings and two phenyl rings of two ligands are both parallel to each other. The dihedral angle between phenyl ring and pyridine ring from the same ligand is 20.38°. By contrast, in the palladium complex, the hydrogen bond interactions manifested by N–H...O contact of 2.879 Å in-

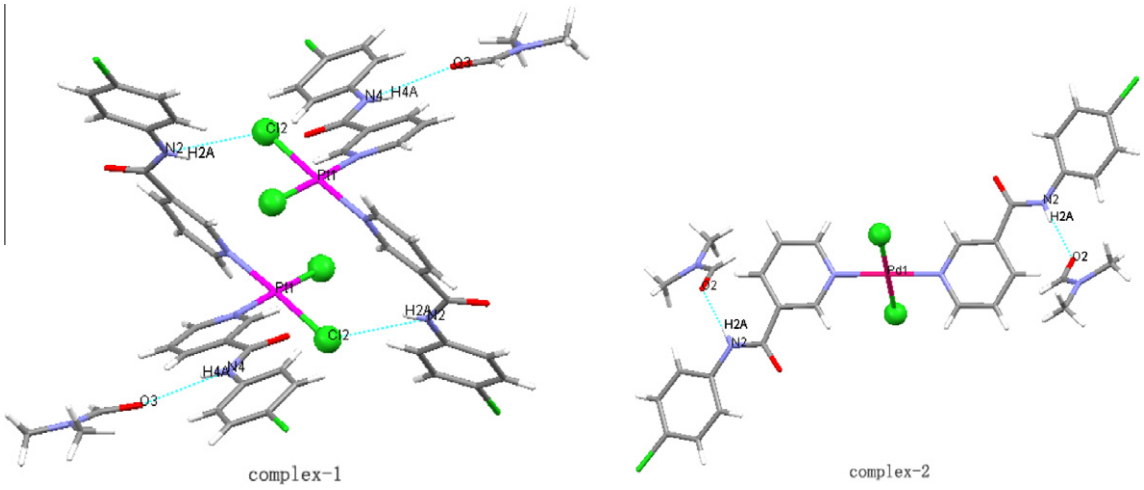

Figure 1. Intermolecular contacts in complexes **1** and **2**.

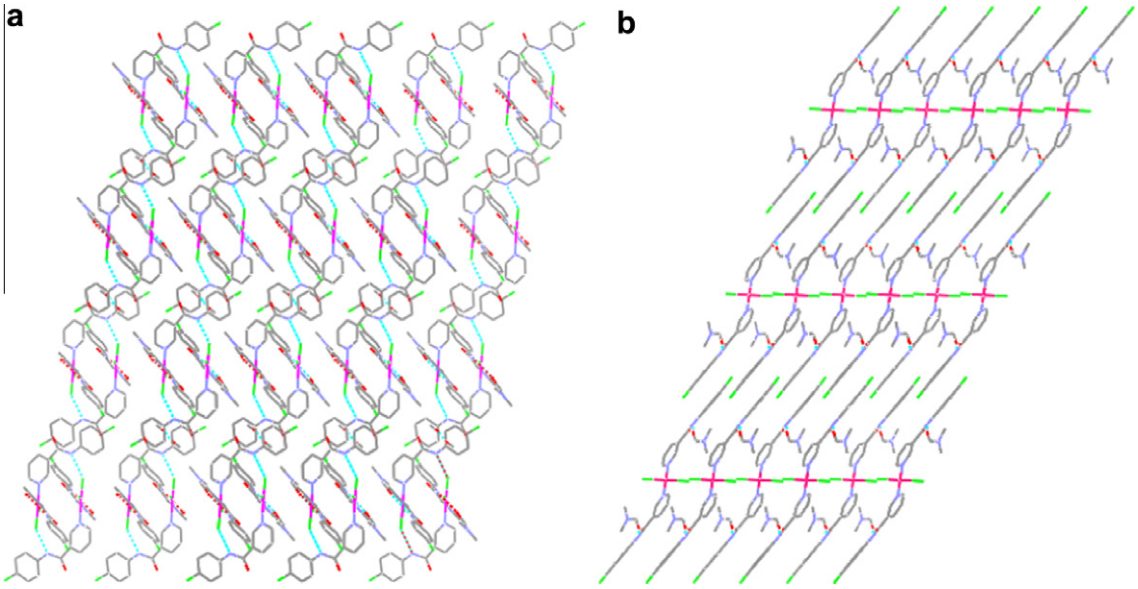

Figure 2. 2D layer-like structure in **1** when viewed down the *c*-axis (a), and in **2** down the *b*-axis (b).

volve the amide nitrogen atoms of ligands and the oxygen atoms of DMF molecules. π–π stacking interactions (amide...pyridine 3.849 Å) between neighbouring molecules which extend in *bc* plane generate a 2D layer-like structure (Fig. 2b). The results showed that the precise structure of the hydrogen bonding network is sensitive to changes in the cis/trans arrangement of complexes and their supramolecular architectures.

Fluorescence quenching measurements have been confirmed to be effective for monitoring the binding nature of the metal complexes to DNA and comparing binding abilities of these complexes. The molecular fluorophore EB (ethidium bromide) has a conjugate planar structure and its fluorescence intensity is very weak, but it emits intense fluorescence at about 600 nm in the presence of DNA due to its strong intercalation between the adjacent DNA base pairs. In previous studies, the enhanced fluorescence of DNA–EB complex could be quenched by the addition of a competing metal complex. This is evidence that the complexes intercalate to base pairs of DNA.[23–25] Figure 3a and b showed the intensity of emission spectra of DNA–EB system decreased with increasing amount of the Pt(II) and Pd(II) complex, respectively. These results indicated that EB was partially replaced by the complexes intercalating into the DNA. According to linear Stern–Volmer equation:[26] $I_0/I = 1 + K_{sq}r$, K_{sq} (the quenching constant) was obtained as the slope of I_0/I versus r linear plot. r is the concentration ratio of the complex to DNA. From the inset in Figure 3, the K_{sq} values for the Pt(II) and Pd(II) complexes were 0.98 and 0.22, respectively. The data suggested that the interaction of complex **1** with DNA was stronger than that of complex **2**. The binding affinity of complexes are probably attributed to the extension of the π system of the intercalated ligand due to the co-ordination of metal ion, which also leads to a planar area of the complex **1** greater than that of the complex **2**, which leads to the co-ordinated ligand penetrating more deeply into, and stacking more strongly with the base pairs of the DNA.[27] In general, it can be confirmed that the reactions of the two intercalatory complexes between the adjacent DNA base pairs have taken place.

The fluorescence Scatchard plot is an important tool to determine how the complex binds to FS-DNA, which can provide the binding mode of the complex to DNA. To get a better insight into the nature of complex-DNA-binding, we have carried out a fluorescence study of EB to DNA in the presence of a competing metal complex. The characteristics of the binding of EB to DNA can be expressed by Scatchard equation:[28]

$$r_E/C_E = K(n - r_E)$$

Here, r_E is the ratio of bound EB to total nucleotide concentration; C_E is the concentration of free EB, n is the number of binding sites per nucleic acid and K is the intrinsic binding constant for EB. The fluorescence Scatchard plots obtained for competition of the complexes with EB to bind with DNA are given in Figure 4. The binding parameters for fluorescence Scatchard plots of FS–DNA with EB in the presence of complexes are shown in Table 1. Both complexes **1** and **2** produce a Scatchard plot in which the slope decreases in the presence of increasing amounts of complex, with little change in the intercept on the abscissa ($0.205 < x_1 < 0.213$, $0.195 < x_2 < 0.217$), which indicates that the two complexes exhibit typical type A behaviour.[28] Thus, it shows typical competitive inhibition of EB binding for both the slope, that is, K change with the increase in the concentrations of the complexes as given in Figure 4 and Table 1, while the intercept of the abscissa, that is, n (number of binding sites per nucleotide) hold within the range. These data indicate that the complex may bind to DNA by the intercalative binding mode. The result provides a further support that the binding modes of the Pt/Pd(II) complexes are intercalative in the interactions with FS-DNA.

Further analysis of data led us to suspect that the complexes intercalate deeply into the DNA base pairs. In addition, there is also evidence that DNA-binding is dependent on the co-ordinated metal centre. The Pt(II) complex is of higher binding affinity to DNA than the Pd(II) complex. This can be rationalised by a consideration of the ionic potential of the co-ordinated metal ion, which is responsible for the geometry of complexes, also affects the intercalating ability of metal complexes to DNA.

The influence of the complexes on the tertiary structure of DNA is evaluated by their DNA-cleavage ability,[29–31] which can be achieved by monitoring the transition from the closed circular supercoiled form (Form I) to the open circular relaxed form (Form II). This occurs when one of the strands of the plasmid is nicked. Figure 5 showed the result of gel electrophoretic separations of plasmid pBR322 DNA after incubation with the two complexes. Lane 0 applied to the untreated pBR322 DNA that acted as control. In the lane 0, pBR322 DNA showed two clear bands, corresponding

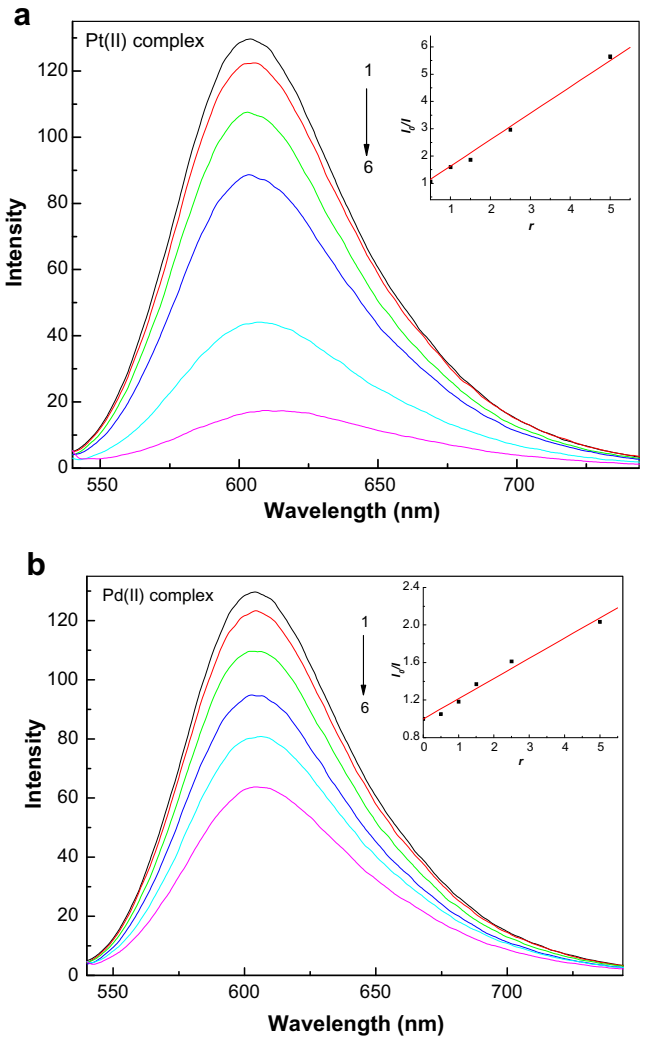

Figure 3. Fluorescence spectra of the binding of EB to DNA in the absence (1) and presence (2–6) of increasing amounts of the complexes λ_{ex} = 525 nm, C_{EB} = 1.0 μM, C_{DNA} = 5.1 μM, $C_{M(1-2)}$ (2–6): 2.5, 5.0, 7.5, 12.5, 25 (μM). (a: complex **1**; b: complex **2**). The inset is Stern–Volmer quenching plots.

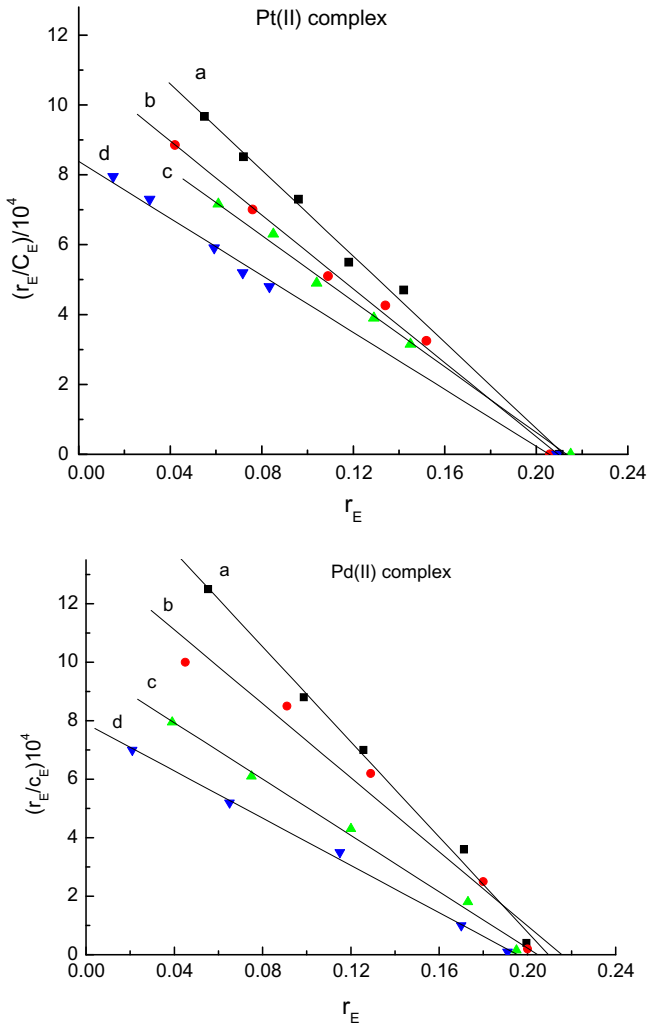

Figure 4. Fluorescence Scatchard plots for the binding of EB (0.5–5 μM) to DNA in the absence (a) and the presence (b–d) of increasing concentrations of complex. r_f increases in the range of 0.000–2.216 for the two complexes. (r_f is the formal ratio of metal complex to nucleotide concentration, r_E is the ratio of bound EB to total nucleotide concentration.)

to Forms I and II, as it was expected. Under comparable experimental conditions, the progressions of the cleavage reactions with different concentrations (6.6 μM and 3.3 μM) of each complex were given in lanes 1 and 2 for complex **1** and 3, 4 for complex **2**. It is clearly seen that the two complexes can induce the obvious cleavage of the plasmid DNA since the intensity of Form II band increases markedly with a corresponding decrease in the intensity of Form I band (lanes 1–4). Meanwhile, cleavage ability of the Pt(II) complex was better than that of the Pd(II) complex. On the other hand, each complex also showed more efficient cleavage activity at the higher concentration (6.6 μM) in comparison to the lower concentration (3.3 μM). All in all, the cleavage efficiency observed from Figure 5 follows the order: lane 1 > 2 > 3 > 4. The change in mobility of Form I DNA band with the increase in concentration of complexes is due to unwinding of the supercoiled Form I DNA. The increase in intensity of the Form II band (as compared to that in the untreated DNA) with the increase in concentration of the complexes is believed to be due to partial nicking of Form I DNA to produce Form II DNA.[32] As a result, there is a wide distribution of relaxed forms (forms topoisomers) that are relaxed to varying extent. Complexes **1** and **2** are believed to form monofunctional adducts with Guanine. The monofunctional adducts could close to form initially bifunctional interstrand GC adducts that can evolve into interstrand GG adducts. When bifunctional interstrand adduct is formed, planar ligand will be positioned along the helix axis so that they will push apart adjacent base pairs.[32] Therefore, these phenomena here imply that the two complexes can bind to and cleave DNA efficiently.

The effects of the two complexes on cell viability were tested using the MTT assay. IC_{50} values were determined and listed in

Table 1
Binding parameters for fluorescence Scatchard plot of FS-DNA with EB in the presence of complex **1** or **2**

Complex	r_f	K_{obs} ($\times 10^5$ M^{-1})	n
1	0.000 ± 0.005	6.1	0.212 ± 0.001
	0.172 ± 0.010	5.3	0.209 ± 0.002
	1.268 ± 0.010	4.7	0.213 ± 0.003
	2.216 ± 0.020	4.1	0.205 ± 0.002
2	0.051 ± 0.005	8.1	0.209 ± 0.001
	0.109 ± 0.012	6.3	0.215 ± 0.001
	1.030 ± 0.010	4.8	0.205 ± 0.002
	2.060 ± 0.015	4.1	0.195 ± 0.003

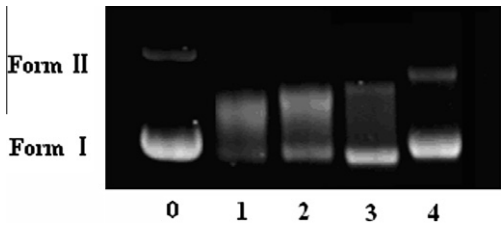

Figure 5. Electrophoretograms for interaction of pBR322 DNA with different concentrations(6.6 μM and 3.3 μM) of complex **1** (lanes 1 and 2) and complex **2** (lanes 3 and 4), respectively. Lane 0 applies to untreated DNA.

Table 2
Cytotoxicity of the complexes against selected human tumour cells after 72 h of incubation (data are expressed as mean ± SD (n = 4))

Complex	In vitro activity (IC_{50} ± SD, μM)			
	Hela	Hep-G2	KB	AGZY-83a
Complex **1**	1.34 ± 0.26	4.12 ± 0.72	2.68 ± 0.61	2.54 ± 0.49
Complex **2**	2.36 ± 0.32	4.76 ± 0.96	3.97 ± 0.74	3.27 ± 0.64
Cisplatin	0.96 ± 0.12	3.64 ± 0.72	1.64 ± 0.73	2.03 ± 0.53

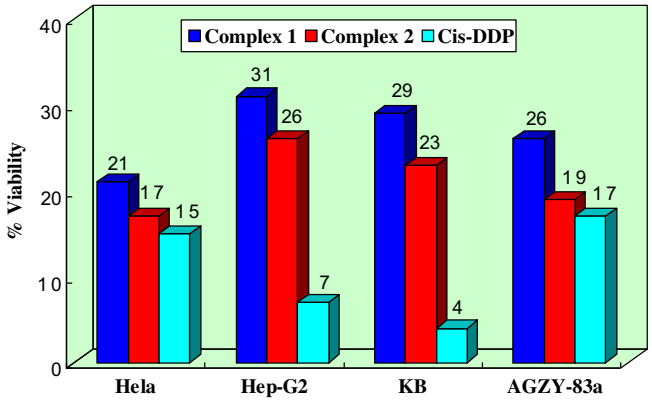

Figure 6. Effect of 3 μg/mL of the complex on cancer cells viability after 72 h of incubation. All determinations are expressed as percentage of the control (untreated cells).

Table 2. The result indicates that **1** and **2** have certain effect on cancer cells and exhibit cytotoxic activity toward the tested human tumour cell lines in comparison to cisplatin, especially against Hela cells. In addition, Figure 6 reveals the effect on cell growth after a treatment period of 72 h treatment with 3 μg/mL concentration. A viability rate by 72 h to <50% of the control values was observed for the complexes. The complexes were more effective in arresting the growth of Hela than other lines. The results coincide with IC_{50} values reveals. The activity differences between complexes **1** and **2** may be correlated to the geometrical differences between them. The result confirms the importance of cis geometry among this new class of complexes. The *trans*-Pd(II) analogue displayed an in vitro anti-tumour activity lower than the corresponding *cis*-Pt(II) complex.

In summary, two novel complexes *cis*-$[PtL_2Cl_2]\cdot CH_3OH\cdot DMF$ (**1**) and *trans*-$[PdL_2Cl_2]\cdot 2DMF$ (**2**) with pyridine carboxamide ligand have been synthesized and characterised. The crystal structure of them were determined by single crystal X-ray diffraction. The properties of DNA-binding and cleaving by the two complexes have also been studied. The results indicate that **1** and **2** can bind to FS-DNA and their binding strengths increase in the order **1** > **2**. The DNA-cleavage studies support the fact that they have the ability to cleave pBR322 DNA. Furthermore, the biological activities in vitro show that the two complexes possess good cytotoxic activity against four different cell lines, especially more effective against Hela cell lines. The presented *cis*-Pt(II) complex shows better anti-tumour activity and DNA-binding characteristics than the *trans*-Pd(II) complex due to the different co-ordination metal centre and geometry of the two complexes. These initial studies are promising and may shed some light on designing new potential anticancer agents and DNA probes in the future.

Acknowledgements

This work is supported by the National Natural Science Foundation of China(no. 20671064, 20971090), Foundation of Educational Department of Liaoning Province (no. 20060679) and the Natural Science Foundation of Liaoning Province (no. 20052014).

Supplementary data

CCDC 776692 (complex **1**) and 739075 (complex **2**) contain the supplementary crystallographic data for this Letter. These data can be obtained free of charge from The Cambridge Crystallographic Data Centre via www.ccdc.cam.ac.uk/data_request/cif. Experimental methods and procedures are available. Supplementary data associated with this article can be found, in the online version, at doi:10.1016/j.bmcl.2010.10.097.

References and notes

1. Sigel, H.; Martin, R. B. *Chem. Rev.* **1982**, *82*, 385.
2. Clement, O.; Rapko, B. M.; Hay, B. P. *Coord. Chem. Rev.* **1998**, *170*, 203.
3. Belda, O.; Moberg, C. *Coord. Chem. Rev.* **2005**, *249*, 727.
4. Kurosaki, H.; Sharma, R. K.; Aoki, S.; Inoue, T.; Okamoto, Y.; Sugiura, Y.; Doi, M.; Isida, T.; Otsuka, M.; Goto, M. *J. Chem. Soc., Dalton Trans.* **2001**, 441.
5. Liu, S.; Luo, Z.; Hamilton, A. D. *Angew. Chem., Int. Ed.* **1997**, *36*, 2678.
6. Lebon, F.; Ledecq, M.; Dieu, M.; Demazy, C.; Remacle, J.; Lapouyade, R.; Kahn, O.; Durant, F. *J. Inorg. Biochem.* **2001**, *86*, 547.
7. Yang, T.; Zhang, J. Y.; Tu, C.; Lin, J.; Liu, Q.; Guo, Z.-J. *Chin. J. Inorg. Chem.* **2003**, *19*, 45.
8. Zhang, J.; Liu, Q.; Duan, C.; Shao, Y.; Ding, J.; Miao, J.; You, X.; Guo, Z. *J. Chem. Soc., Dalton Trans.* **2002**, 591.
9. Noveron, J. C.; Lah, M. S.; Del Sesto, R. E.; Arif, A. M.; Miller, J. S.; Stang, P. J. *J. Am. Chem. Soc.* **2002**, *124*, 6613.
10. Zhang, J. Y.; Ke, X. K.; Tu, C.; Lin, J.; Ding, J.; Lin, L. P.; Fun, H. K.; You, X. Z.; Guo, Z. J. *Biometals* **2003**, *16*, 485.
11. He, X. Q.; Lin, Q. Y.; Hu, R. D.; Lu, X. H. *Spectrochim. Acta, Part A* **2007**, *68*, 184.
12. Rosenberg, B.; Camp, L. V.; Krigas, T. *Nature* **1965**, *205*, 698.
13. Beusichem, M. V.; Farrell, N. *Inorg. Chem.* **1992**, *31*, 634.
14. Coluccia, M.; Nassi, A.; Loseto, F.; Boccarelli, A.; Mariggio, M. A.; Giordano, D.; Intini, F. P.; Caputo, P. A.; Natile, G. *J. Med. Chem.* **1993**, *36*, 510.
15. Natile, G.; Coluccia, M. *Coord. Chem. Rev.* **2001**, *216–217*, 383.
16. Radulovic, S.; Tesic, Z.; Manic, S. *Curr. Med. Chem.* **2002**, *9*, 1611.
17. Beck, W. M.; Calabrese, J. C.; Kottmair, N. D. *Inorg. Chem.* **1979**, *18*, 176.
18. Beer, P. D.; Fletcher, N. C.; Drew, M. G. B.; Wear, T. J. *Polyhedron* **1997**, *16*, 815.
19. Qin, Z.; Jennings, M. C.; Puddephatt, R. J. *Inorg. Chem.* **2001**, *40*, 6220.
20. Szüčová, L.; Trávníček, Z.; Zatloukal, M.; Popa, I. *Bioorg. Med. Chem.* **2006**, *14*, 479.
21. Huq, F.; Tayyem, H.; Beale, P.; Yu, J. Q. *J. Inorg. Biochem.* **2007**, *101*, 30.
22. Shi, C. Y.; Ge, C. H.; Gao, E. J.; Yin, H. X.; Liu, Q. T. *Inorg. Chem. Commun.* **2008**, *11*, 703.
23. Sun, Y. T.; Bi, S. Y.; Song, D. Q.; Qiao, C. Y.; Mu, D.; Zhang, H. Q. *Sens. Actuators, B* **2008**, *129*, 799.
24. Gao, E. J.; Wang, K. H.; Gu, X. F.; Yu, Y.; Sun, Y. G.; Zhang, W. Z.; Yin, H. X.; Wu, Q.; Zhu, M. C.; Yan, X. M. *J. Inorg. Biochem.* **2007**, *101*, 1404.
25. Gao, E. J.; Liu, L.; Shi, C. Y.; Yin, H. X.; Zhu, M. C.; Wu, Q.; Liu, Q. T. *Chin. J. Chem.* **2009**, *27*, 1061.
26. Lakowicz, J. R.; Weber, G. *Biochemistry* **1973**, *12*, 4161.
27. Wang, B. D.; Yang, Z. Y.; Li, T. R. *Bioorg. Med. Chem.* **2006**, *14*, 6012.
28. Howe-Grant, M.; Wu, K. C.; Bauer, W. R.; Lippard, S. J. *Biochemistry* **1976**, *15*, 4339.
29. Gao, E. J.; Zhu, M. C.; Liu, L.; Huang, Y.; Wang, L.; Shi, C. Y.; Zhang, W. Z.; Sun, Y. G. *Inorg. Chem.* **2010**, *49*, 3261.
30. Gao, E. J.; Zhu, M. C.; Huang, Y.; Liu, L.; Liu, H. Y.; Liu, F. C.; Ma, S.; Shi, C. Y. *Eur. J. Med. Chem.* **2010**, *45*, 1034.
31. Gao, E. J.; Shi, Q. Z.; Zhu, M. C.; Liu, L.; Shi, C. Y.; Zhang, W. Z. *Chin. J. Chem.* **2009**, *27*, 2341.
32. Chowdhury, M. A.; Huq, F.; Abdullah, A.; Beale, P.; Fisher, K. *J. Inorg. Biochem.* **2005**, *99*, 1098.